Fluorescence Characteristics of Highly-Pure Nanoparticles Embedded in Dye Complexes for Random Laser Design

Atheer A. Mahmood
Al Iraqia University
Oday A. Hammadi (odayata2001@yahoo.com)
Al Iraqia University
Kais R. Ibraheem
University of Anbar

Research Article

Keywords: Metal complex, Fluorescence, Photoluminescence, Nanoparticles, Random laser

Posted Date: December 9th, 2021

DOI: https://doi.org/10.21203/rs.3.rs-1149737/v1

Abstract

In this work, highly-pure titanium dioxide nanoparticles produced by dc magnetron sputtering technique were embedded in organometallic complex solutions such as Baq_2 or Znq_2 to form random gain media. The structural characteristics of the TiO_2 nanoparticles were determined to confirm their high structural purity. The spectroscopic characteristics, mainly photoluminescence and fluorescence, of the complex solutions containing the nanoparticles were determined and studied. These media were compared to two of the most common laser dyes (Rhodamine b and Rhodamine 6G) to determine the feasibility to use them to produce random laser.

1. Introduction

Recently, fluorescence has become one of the most important techniques in characterization and diagnosis in applied and experimental sciences due to its sensitivity, ease of use, and versatility [1]. Fluorescence is the emission of light from any substance and occurs from electronically excited singlet states. Emission of light from triplet excited states is phosphorescence. Absorption of photons will excite a fluorophore into singlet excited states. This process is so fast and occurs within 10^{-15} s. Quick internal conversion (10^{-12} s) gets the fluorophore to the lowest vibrational level [2].

Intensive fluorescence showed nonfluorescent throw metal complexes of oxine and its derivatives excluding in concentrated sulfuric and perchloric [3, 4]. Fluorescence features of hydroxyquinoline with metals have been hard-done by leadership act in paper chromatography by Feigl and Heisig [5].

Nanoparticles of metals are recognized to significantly modify the spontaneous emission of close by fluorescent molecules and materials [6]. The metal chelates of 8-hydroquinoline arouse wide interesting because of their novel structure and fluorescence characteristics [7, 8]. The role of Nano sized gold on fluorescence properties of Rh6G has been analyzed by using steady state and time resolved fluorescence methods [9].

Nanoparticles have acquired intensive interest in biology and medication because of their particular electric, optical, and catalytic properties [10–14].

Bis(8-hydroxyquinoline) zinc has been provided to be useful for excessive efficiency working voltage OLEDs [15–17].

Nanoparticles of metal oxide have attracted factors in present years because of their large ranging programs in environmental remediation and digital devices. They had been broadly utilized in solar cells, piezoelectric nanogenerators, optoelectronic devices, UV detectors, photocatalysis, etc. due to their extended bandgap, insolubility, and small sizes [18-22].

Titanium dioxide for photocatalytic uses due to its numerous advantages, which consist of a large chemical and optical stabilities, low charge and low toxicity [23,24].

2. Experimental Part

Complexes had been synthesized as adding 2.9 g of 8-hydroxyquinoline which was dissolved in a mixture of (potassium hydroxide 1.12 g with distilled water) then it was stirred well. A 1.36 g sample of every salt ($BaCl_2.2H_2O$ and $ZnCl_2$) were dissolved in distilled water and stirred well. Theses aqueous solutions were mixed with solution in the first step and the remaining combination mixture with stirring for 20 min. Each complex was prepared by 1:2 ratios. Finally, product was dried at oven for six hours after washing in distilled water.

In order to form the random gain media, highly-pure titanium dioxide nanoparticles with average particle size of 25 nm were added to the complex solution and the absorption and photoluminescence spectra were recorded and compared before and after adding these nanoparticles. The minimum amount of added nanoparticles was 0.5 mg for 5 mL of complex solution of 10^{-5} M concentration. Many experiments were carried out to determine these preparation conditions.

The ligands and synthesized complexes were characterized as follows. The absorption spectra were recorded using UV-Visible SPEKOL 2000 double-beam spectrophotometer supplied by PG Instruments (UK), which has a slit width in a spectral range of 190-1100 nm. UV-visible measurements were performed on the samples in ethanol. The field-effect scanning electron microscopy (FE-SEM) was used to study the effect of nanoparticle size and distribution on the characteristics of the prepared samples. The photoluminescence (PL) properties of complexes were measured by Hitachi F-7000f fluorescence spectrometer with 150 W monochromatic xenon lamps as the excitation source.

In this work, a dc reactive magnetron sputtering system was used. A highly-pure titanium sheet with 10cm diameter was used as a target to be mounted on the cathode by a Teflon flange. The uncovered area is about 8cm in diameter. Also, highly-pure argon and oxygen gases were used as discharge and reactive, respectively. Borosilicate glass slides are used as substrates after been cleaned with ethanol and distilled water and dried before placed on the anode surface.

The deposition chamber is initially evacuated down to 10^{-3} mbar to exclude any residuals and contaminants. Meanwhile, the argon and oxygen gases are mixed in the gas mixture with the required mixing ratio. Then, the gas mixture is pumped into the chamber with a controllable flow rate using needle valve. The dc power supply is operated and the applied voltage is gradually increased until the plasma appears due to the breakdown of argon at about 190 V. As soon as the plasma column is formed, the sputtering process starts where the positive ions of plasma (Ar^+) hit the target to sputter atoms from its surface. These sputtered atoms move in the opposite direction (towards the anode) and pass through the oxygen gas species. Here, some atoms are bonding to the oxygen forming metal oxide molecules and then deposit on the substrate placed on the surface of anode. The operation parameters were optimized and more details can be found elsewhere [25-29]. The nanopowder was extracted from the titanium dioxide thin film samples prepared in this work by ultrasonic waves-assisted conjunctional freezing technique [30,31].

By controlling deposition time, the film thickness can be controlled. However, the optimum samples were prepared using gas mixing ratio (Ar:O_2) of 1:1, inter-electrode distance of 4 cm, and deposition time of two hours. The structural and spectroscopic characteristics of these samples were determined by x-ray diffraction (XRD), scanning electron microscopy (SEM), energy-dispersive x-ray spectroscopy (EDX), UV-visible and Fourier-transform infrared (FTIR) spectroscopy, fluorescence and photoluminescence spectroscopy.

3. Results And Discussion

Figure (2) shows the XRD pattern of TiO_2 thin film sample prepared in this work. It is clear that the sample exhibits high structural purity as no peaks belonging to other materials than TiO_2 are observed. In TiO_2 sample, both phases (rutile; R and anatase; A) are recognized [(32)], however, the anatase phase is apparently dominant as the crystal planes belonging to anatase TiO_2 are more than those belonging to rutile TiO_2.

Further confirmation of the structural purity of the prepared samples can be presented by the FTIR results shown in Fig. (3). The main peaks belonging to the vibration of Ti-O and O-Ti-O are observed with additional peaks belonging to the O-H group, which are resulted from the exposure to the environment [33-36]. Therefore, the prepared sample can be described as highly-pure.

Surface profile and particle size for the prepared thin films were determined by scanning electron microscopy (SEM). The SEM image of TiO_2 nanopowder extracted from thin film sample prepared in this work using Ar:O_2 mixture of 50:50 mixing ratio and inter-electrode distance of 4 cm after deposition time of one hour is shown in Fig. (4). The first feature can be seen in these images is the homogeneity of particle distributions, which is one of the most important advantages of dc magnetron sputtering technique used for synthesis of nanostructures. Another important feature can be seen is the absence of aggregation over the scanned sample. In the mixed-phase TiO_2 sample prepared in this work, the 13 crystal planes can form intertwined facets and hence the inter-space between nanoparticles may be minimized and the nanosurface show much more flatness than in the single-phase sample [37]. A minimum particle size of about 40 nm can be seen while no large aggregation is observed. The energy-dispersive x-ray (EDX) spectrum for titanium dioxide nanopowder extracted from this thin film sample is shown in Fig. (5). The summary of elemental compositions in the final samples is presented in the table below the figure. With the existence of Ti and O in the final sample, the percentage weights of Ti and O was found to be 46.77 and 50.79, respectively. This result confirmed the stoichiometry of the TiO_2 molecules as it completely agrees with the chemical bonding configuration of such compound. In this sample, no impurities were detected as supported by the atomic integration of Ti and O elements. This feature is highly preferred for studies concerned to the concepts of physical and chemical characteristics and processes [29].

The absorption spectra of the two complexes were organized before and after adding nanoparticles to the complexes in ethanol solvent. It is apparent that the absorption peak for Baq_2 complex at 326 nm, changed after adding the nanoparticles. However, all complexes confirmed high absorbance in the ultraviolet region (<300nm) after adding the nanoparticles. As well, the Baq_2 complex confirmed higher absorbance in the spectral range 500-800 nm after adding the nanoparticles even as the distinction in very small absorbance for Znq_2 complex. As the good result of the organometallic complexes organized as the random gain media, then their photoluminescence spectra were recorded and compared before and after adding the nanoparticles, as shown in Fig. (6).

All complexes confirmed distinct peaks; the primary in the blue region (450-470nm) and the second one in the region (510-515nm). In the Baq_2 complex, the width of the primary peak changed into better than that of the second one, in comparison to the Znq_2 wherein the width of the second one peak changed into better than that of the primary one.

Photoluminescence (PL) spectroscopy is a form of light emission spectroscopy in which the light emission originates from a process called photo-excitation. As the light is directed onto a sample, the electrons within the material move into excited states. When the electrons come down from the excited states to their equilibrium states, the energy can be released in the form of light.

The absorbance spectrum is created by exciting electrons at varying wavelengths while monitoring the emission at a fixed wavelength. The results from an absorbance spectrum is valuable in determining the fixed excitation wavelength for the emission spectrum.

In order to determine the effect of nanoparticles on the main spectroscopic characteristics of the prepared dye complexes, the photoluminescence (PL) spectra of each complex prepared in this work were recorded before and after adding the TiO_2 nanoparticles to the solution of the prepared complex in the spectral range of 250-750 nm, as shown in Fig. (7).

For the Baq_2 complex, it is clear that adding the nanoparticles results in an increase in the PL intensity at the same peak of the Baq_2 alone (457nm) as shown in Fig. (7a). This increase is slight (~2.4%), however, an increase up to 23% was observed at 661 nm, which is reasonably lower than the peak wavelength. This increase is attributed to the role of nanoparticles added to the complex solution as they provide more excited states for electrons to reach as a result of photoexcitation. The photoluminescence of this medium (Baq_2+NPs) certainly will be higher than that of Baq_2 only. Similar behavior was observed in Znq2 complex solution containing TiO_2 nanoparticles as the photoluminescence intensity at the peak wavelength (471nm) was higher than that of Znq_2 only at the same wavelength as shown in Fig. (7b). However, the percentage increase in photoluminescence intensity is more than 27% due to adding nanoparticles to the complex solution. This difference in percentage increase may be ascribed to the matching between Znq_2 molecules and TiO_2 nanoparticles, which seems better than that between Baq_2 molecules and TiO_2 nanoparticles.

Since the aim of this work is to synthesize dye complexes for spectroscopic applications, mainly random gain media, then the fluorescence spectra of both complexes (Baq_2 and Znq_2) were compared to some standard laser dyes whose emission ranges are close to those of the complexes as much as possible. Therefore, the fluorescence spectrum of the Baq_2 was compared to that of Rhodamine B dye while the fluorescence spectrum of the Znq_2 complex was compared to that of Rhodamine 6G dyes, as shown in Fig. (8).

As can be seen in Fig. (8a), the maximum of fluorescence intensity of the Baq_2 complex is about 43% of that of Rhodamine B at the same peak wavelength of 610 nm. Similarly, the maximum of fluorescence spectrum of the Znq_2 complex is about 65% that of Rhodamine 6G at the same peak wavelength of 570 nm as shown in Fig. (8b). Also, the spectral width for both complexes (Baq_2 and Znq_2) is reasonably larger than that of laser dyes (RB and R6G, respectively). This width can be narrowed using optical components such as etalons when the complex is employed as a laser active medium.

In order to fabricate random gain media from the synthesized complexes, highly pure titanium dioxide (TiO_2) nanoparticles were added to each complex, fluorescence spectra were recorded and compared to their spectra before adding these nanoparticles, as shown in Fig. (9).

It can be clearly seen in Fig. (9a) the effect of nanoparticles on the fluorescence spectrum of the Baq_2 complex. This effect is attributed to the drastic increase in absorption and hence in fluorescence because the nanoparticles act as trapping centers to the incident photons those would suffer from extremely higher path lengths throughout the complex sample. This certainly increases the probability to absorb more photons and hence the emission is higher in intensity.

On the other hand, the effect of adding nanoparticles to the Znq_2 can be neglected as no variation is observed in the fluorescence spectrum shown in Fig. (9b). this may be attributed to the high absorption of Znq_2 molecules to the incident photons before trapped by the nanoparticles added to the complex sample. Another possible reason is the formation of Zn nanoparticles within the complex, so they play the same role of TiO_2 nanoparticles (as in Baq_2 sample). Therefore, these nanoparticles would not contribute to the emission.

Apparently, the Baq_2 complex solution containing highly pure TiO_2 nanoparticles is better to fabricate random gain media than the Znq_2, while the Znq_2 complex solution is better to replace the Rhodamine 6G in conventional dye laser design.

4. Conclusion

The spectroscopic characteristics of organometallic complexes such as Baq_2 and Znq_2 can be enhanced by adding highly-pure nanoparticles. Such nanoparticles can be efficiently produced by dc magnetron sputtering technique. The effects of adding these nanoparticles to the complex solutions were apparently observed by the enhancement of photoluminescence and fluorescence characteristics. As a conclusion,

the media fabricated from highly-pure TiO_2 nanoparticles embedded in an organometallic complex, such as Baq_2 or Znq_2, can be used to design and fabricate random gain media.

References

[1] Xie, F.; Baker, M. S.; Goldys, E. M. “Enhanced Fluorescence Detection on Homogeneous Gold Colloid Self-Assembled Monolayer Substrates.” Chem. Mater. 2008, 20, 1788-1797.

[2] Lackowicz, J. R. “Principles of Fluorescence Spectroscopy”, 2006, 3rd ed., Springer: New York.

[3] Popovych, O.; Rogers, L. B. Spectrochlm.” Fluorescence in the 8-quinolinol family and the n-π transition“, Acta 1959, 15, 584-592.

[4] Bratzel, M. P.; Aaron, J. J.; Wlnefordner, J. D.; Schulman, S. G.; Gershon, H.” Investigation of excited singlet state properties of 8-hydroxyquinoline and its derivatives by fluorescence spectrometry”, Anal. Chem. 1972, 44, 1240-1245.

[5] Fiegl, F.; Helslg, G. B., “Analytic aspects of the chemical behavior of 8-hydroxyquinoline (oxine), Anal. Chem. Acta 1949, 3, 561-566.

[6] F. Tam, G.P. Goodrich, B.R. Johnson, N.J. Halas, Nano letters, 2007, “Plasmonic enhancement of molecular fluorescence”, 7, 2, 496-501.

[7] Guo. Y.J., “Fluorescence experimental Technology and Its Application in biology”, Science Press. China, 1984.

[8] Prat M.D., Compano R., Beltran J.L. and Condony R., “Fluorescence of Metal Complexes of 8-Hydroxyquinoline Derivatives in Aqueous Micellar Media. J. Fluorescence”. 1994, 4, 4; 279-281.

[9] B. Karthikeyan, “Fluorescence quenching of rhodamine-6G in Au nanocomposite polymers”, J. Appl. Phys., 2010, 108, 084311.

[10] Hussain S, Youngs I J, Ford I J. “The dielectric properties of charged nanoparticle colloids at radio and microwave frequencies”, J Phys, 2004, 37: 318-325.

[11] Goodson T, Varnavski O, Wang Y. “Optical properties and applications of dendrimer–metal nanocomposites”, Int Rev Phys Chem, 2004, 23: 109-150.

[12] Ding Y. S., Shen X. F., Sithambaram S., “Synthesis and Catalytic Activity of Cryptomelane-Type Manganese Dioxide Nanomaterials Produced by a Novel Solvent-Free Method” Chem Mater, 2005, 17: 5382-5389.

[13] Pham-HUU C, Ledoux M J., “Carbon nanomaterials with controlled macroscopic shapes as new catalytic materials”, Top Catal. 2006, 40: 49-63.

[14] Daniel M C, Astruc D., “Gold Nanoparticles: Assembly, Supramolecular Chemistry, Quantum-Size-Related Properties, and Applications toward Biology, Catalysis, and Nanotechnology”, Chem. Rev., 2004, 104: 293-346.

[15] C. H. Chen, J. M. Shi, “Metal chelates as emitting materials for organic electroluminescence”, Coordin. Chem. Rev., 1998, 171, 161.

[16] Y. Hamada et al., “Organic Electroluminescent Devices with 8-Hydroxyquinoline Derivative-Metal Complexes as an Emitter”, Jpn. J. Appl. Phys., 1993, 32, L514.

[17] L. S. Sapochak, F. E. Benincasa, R. S. Schofield, “Electroluminescent Zinc(II) Bis(8-hydroxyquinoline): Structural Effects on Electronic States and Device Performance

”, J. Am. Chem. Soc., 2002, 124, 6119.

[18] M. M. Rahman et al., A comparative study on the photocatalytic degradation of industrial dyes using modified commercial and synthesized TiO2 photocatalysts. J. Chem. Eng., 2014, 27 (2), 65.

[19] 2.A. O. Ibhadon, and P. Fitzpatrick, “Heterogeneous photocatalysis: recent advances and applications”, 2013, Catalysts 3 (1), 189.

[20] 3.A. Gnanaprakasam, V. M. Sivakumar, and M. Thirumarimurugan, Influencing parameters in the photocatalytic degradation of organic effluent via Nano metal oxide catalyst: a review. Indian J. Mater. Sci., 2015, 1.

[21] 4.N. M. Julkapli, S. Bagheri, and S. B. A. Hamid, Recent advances in heterogeneous photocatalytic decolonization of synthetic dyes. Sci. World J. 2014, 1.

[22] 5.A. J. Attia, S. H. Kadhim, and F. H. Hussein, Photocatalytic degradation of textile dyeing wastewater using titanium dioxide and zinc oxide. E J. Chem., 2008, 5 (2), 219.

[23] Wang Q, Yun G, Bai Y, An N, Chen Y, WangR et al 2014 “CuS, NiS as co-catalyst for enhanced photocatalytic hydrogen evolution over TiO_2”, Int. J. Hydrog. Energy 39, 25, 13421-13428.

[24] Yin J, Huang S, Jian Z, Wang Z and Zhang Y 2015 “, Mater. Sci.Semicond. Process. 34, 198.

[25] O.A. Hammadi, M.K. Khalaf, F.J. Kadhim, B.T. Chiad, “Operation Characteristics of a Closed-Field Unbalanced Dual-Magnetrons Plasma Sputtering System”, Bulg. J. Phys., 41(1), 2014, 24-33.

[26] O.A. Hammadi, W.N. Raja, M.A. Saleh and W.A. Altun, “Employment of Magnetron to Enhance Langmuir Probe Characteristics of Argon Glow Discharge Plasma in Sputtering System”, Iraqi J. Appl. Phys., 12(4), 2016, 19-28.

[27] E.A. Al-Oubidy and F.J. Al-Maliki, “Effect of Gas Mixing Ratio on Energy Band Gap of Mixed-Phase Titanium Dioxide Nanostructures Prepared by Reactive Magnetron Sputtering Technique”, Iraqi J. Appl. Phys., 2018, 14(4), 19-23.

[28] F.J. Al-Maliki, O.A. Hammadi and E.A. Al-Oubidy, “Optimization of Rutile/Anatase Ratio in Titanium Dioxide Nanostructures prepared by DC Magnetron Sputtering Technique”, Iraqi J. Sci., 2019, 60 (Special Issue), 91-98.

[29] F.J. Al-Maliki and E.A. Al-Oubidy, “Effect of gas mixing ratio on structural characteristics of titanium dioxide nanostructures synthesized by DC reactive magnetron sputtering”, Physica B: Cond. Matter, 2019, 555, 18-20.

[30] O.A. Hammadi, “Production of Nanopowders from Physical Vapor Deposited Films on Nonmetallic Substrates by Conjunctional Freezing-Assisted Ultrasonic Extraction Method”, Proc. IMechE, Part N, J. Nanomater. Nanoeng. Nanosys, 2018, 232(4), 135-140.

[31] O.A. Hammadi, “Effects of Extraction Parameters on Particle Size of Titanium Dioxide Nanopowders Prepared by Physical Vapour Deposition Technique”, Plasmonics, 2020, 15.

[32] M. Ladd and R. Palmer, “Structure Determination by X-Ray Crystallography”, 5th ed., Springer (NY), 2013, p. 568.

[33] N.N. Greenwood and E.J.F. Ross, “Index of Vibrational Spectra of Inorganic and Organometallic Compounds”, vol. I, Butterworth Group (London), 1960, p. 326, 328.

[34] N.N. Greenwood and E.J.F. Ross, “Index of Vibrational Spectra of Inorganic and Organometallic Compounds”, vol. II, Butterworth Group (London), 1963, p. 457.

[35] N.N. Greenwood and E.J.F. Ross, “Index of Vibrational Spectra of Inorganic and Organometallic Compounds”, vol. III, Butterworth Group (London), 1966, p. 800, 1078.

[36] V.P. Tolstoy, I.V. Chernyshova and V.A. Skryshevsky, “Handbook of Infrared Spectroscopy of Ultrathin Films”, John Wiley & Sons, Inc. (NJ), 2003, p. 435.

[37] B. Roy and S. Aich, "Synthesis of Mixed-Phase TiO2 Powders in Salt Matrix and Their Photocatalytic Activity, Materials and Manufacturing Processes", 2016, Vol. 31, pp. 1628-1633.

Figures

Figure 1

Titanium dioxide nanopowder extracted from thin film samples prepared in this work using Ar:O2 mixture of 50:50 mixing ratio and inter-electrode distance of 4 cm after deposition time of one hour

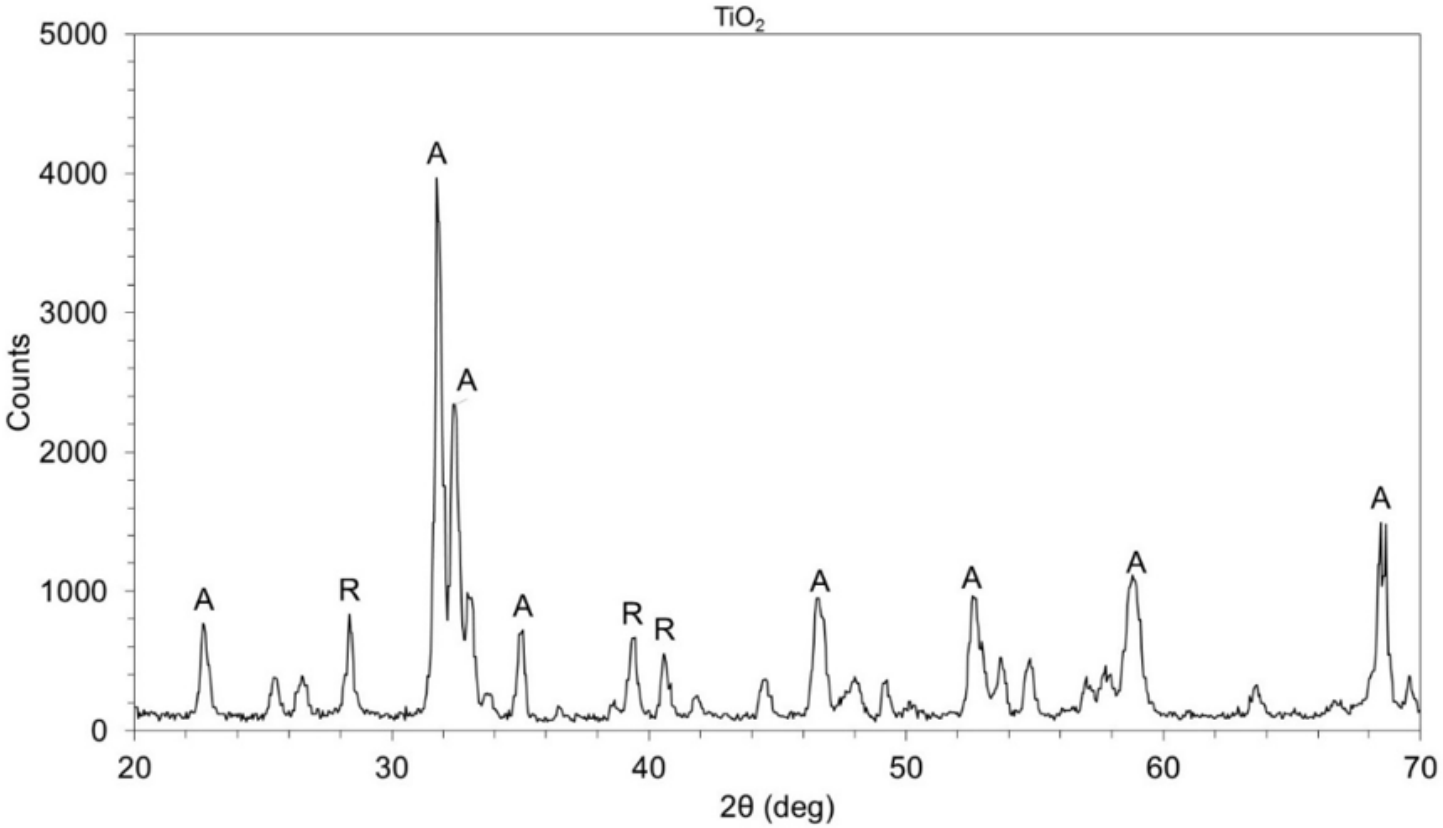

Figure 2

XRD pattern of titanium dioxide nanopowder extracted from thin film samples prepared in this work

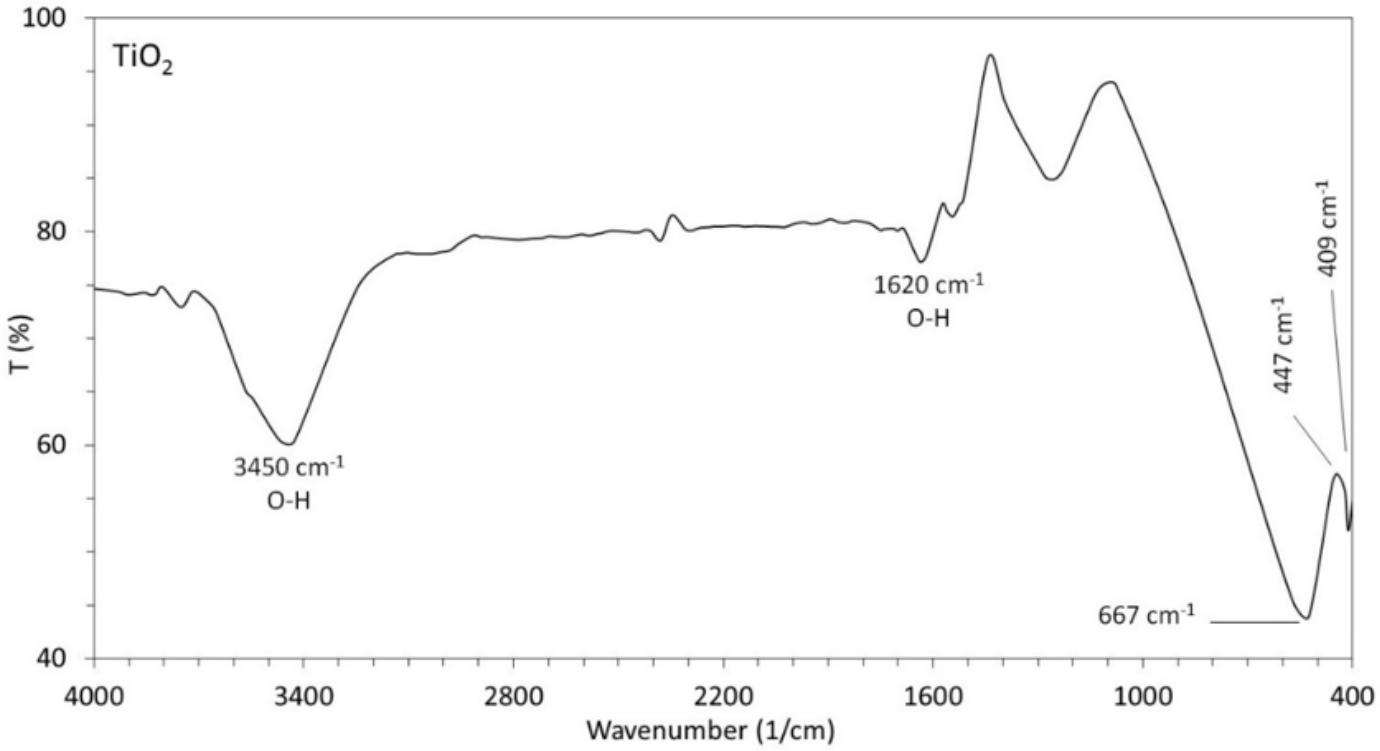

Figure 3

FTIR spectrum of titanium dioxide nanopowder extracted from thin film samples prepared in this work

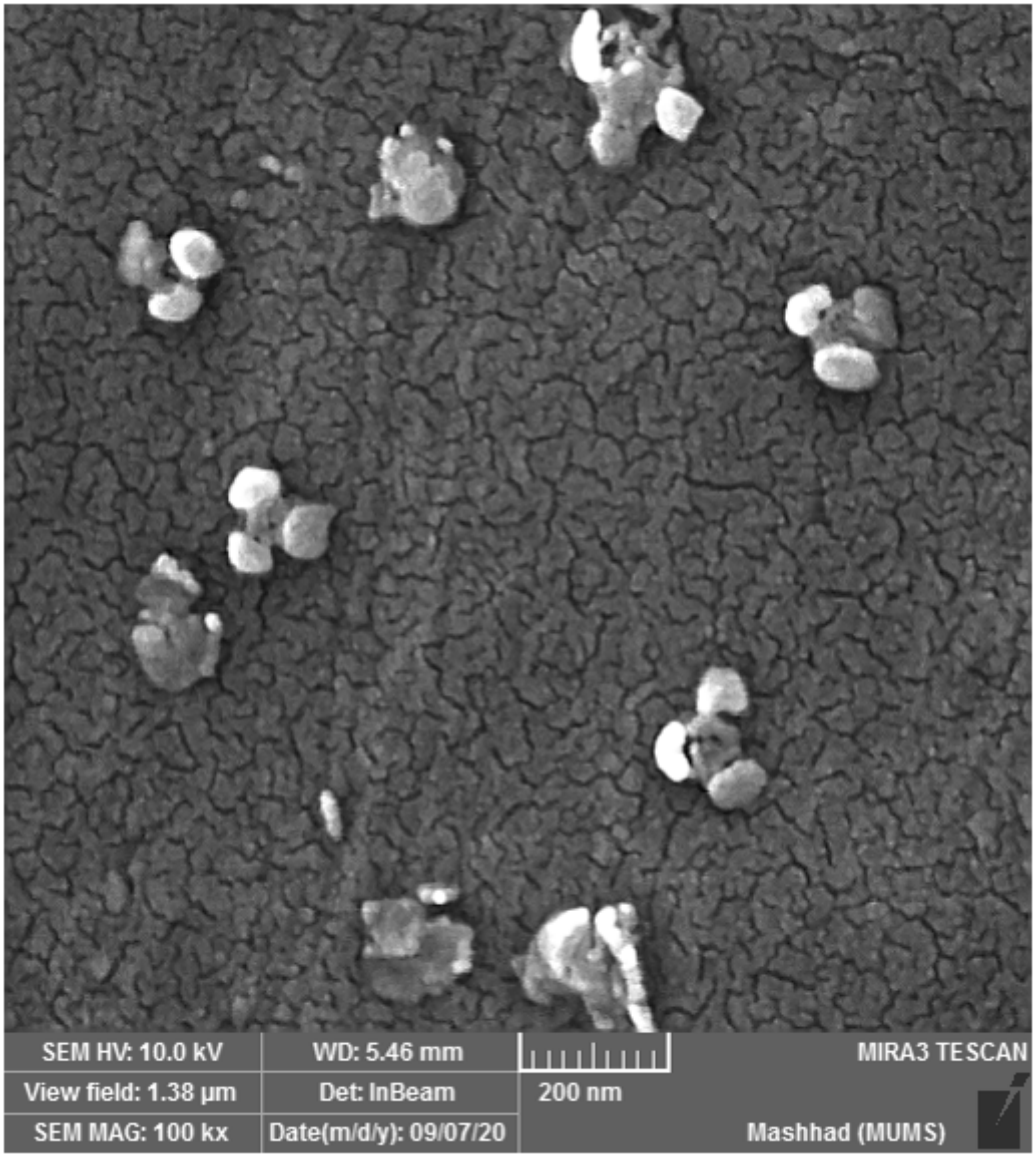

Figure 4

SEM image of titanium dioxide nanopowder extracted from thin film samples prepared in this work

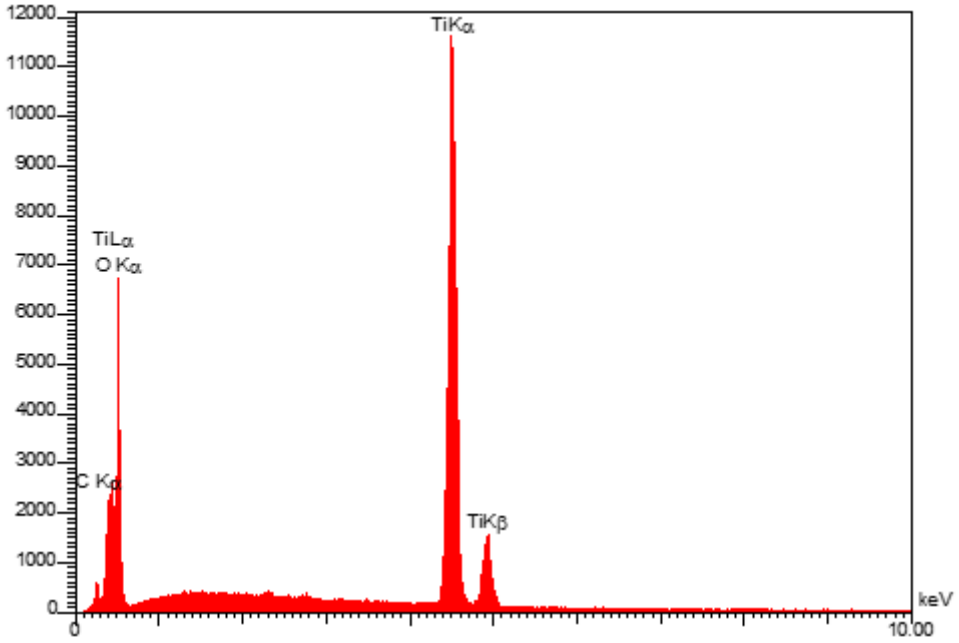

Elt	Line	Int	W%	A%
C	Ka	80.0	2.44	4.67
O	Ka	670.5	50.79	72.91
Ti	Ka	2361.4	46.77	22.42
			100.00	100.00

Figure 5

EDX spectrum of titanium dioxide nanopowder extracted from thin film samples prepared in this work

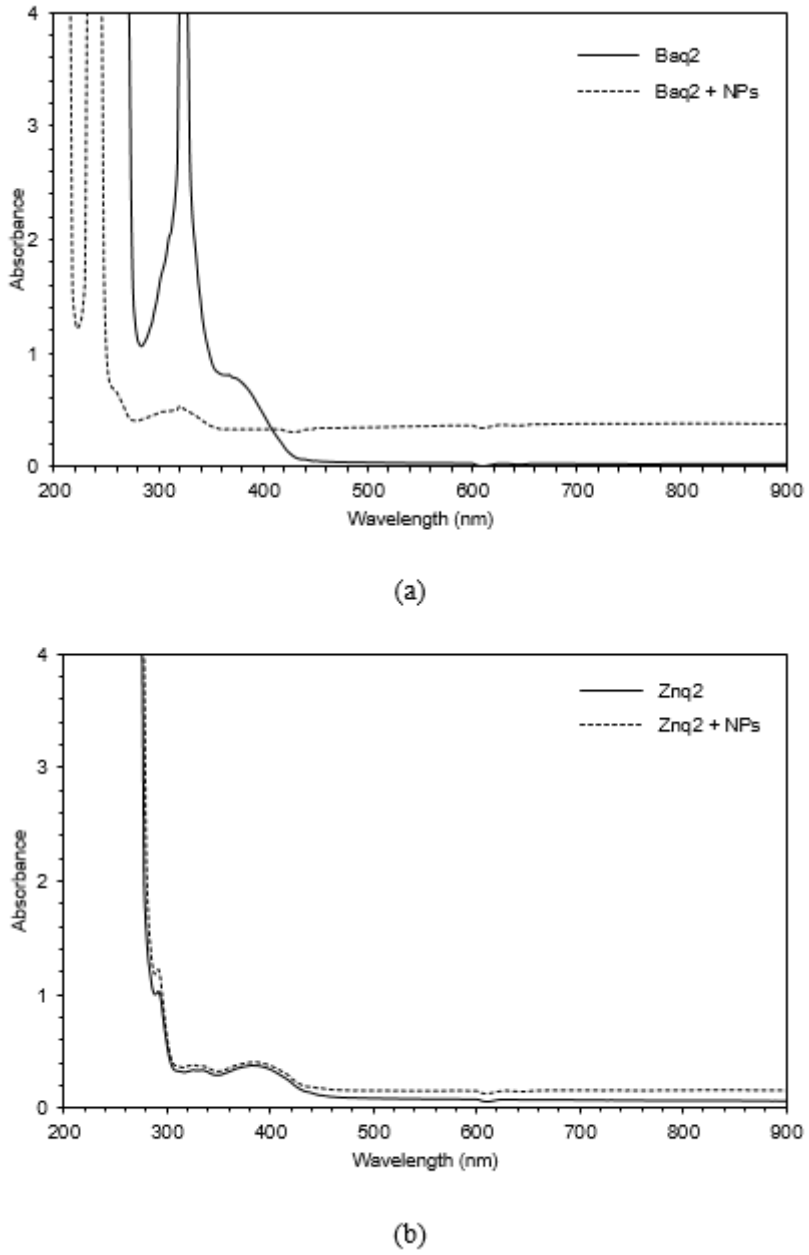

Figure 6

Absorption spectra of Baq2 complex (a) and Znq2 complex (b) prepared in this work before and after adding nanoparticles

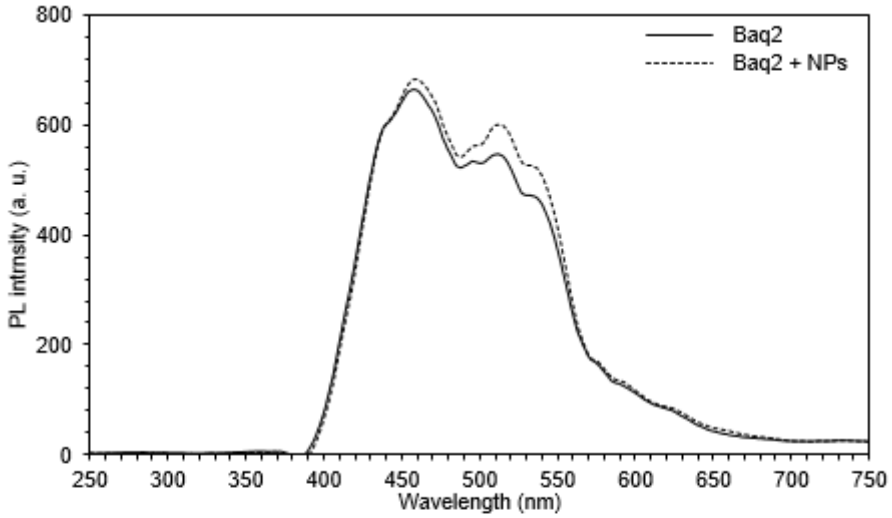

(a)

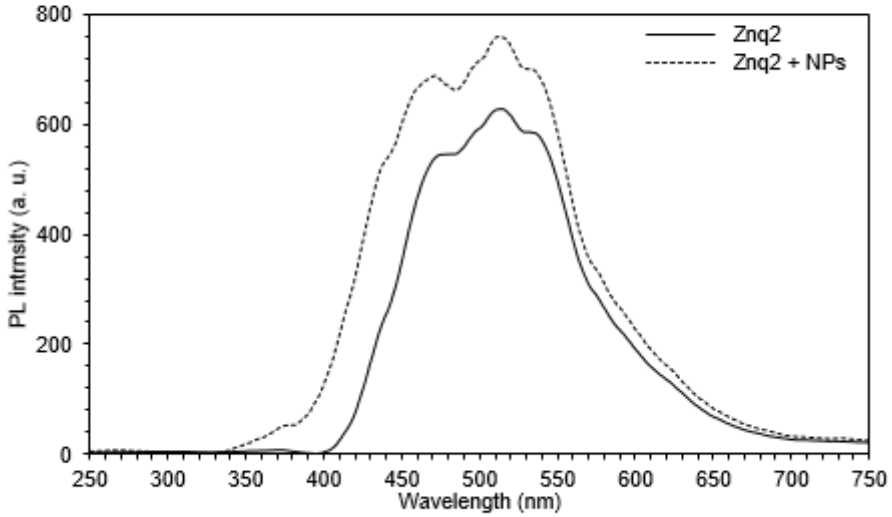

(b)

Figure 7

Photoluminescence spectra of Baq2 complex (a) and Znq2 complex (b) prepared in this work before and after adding nanoparticles

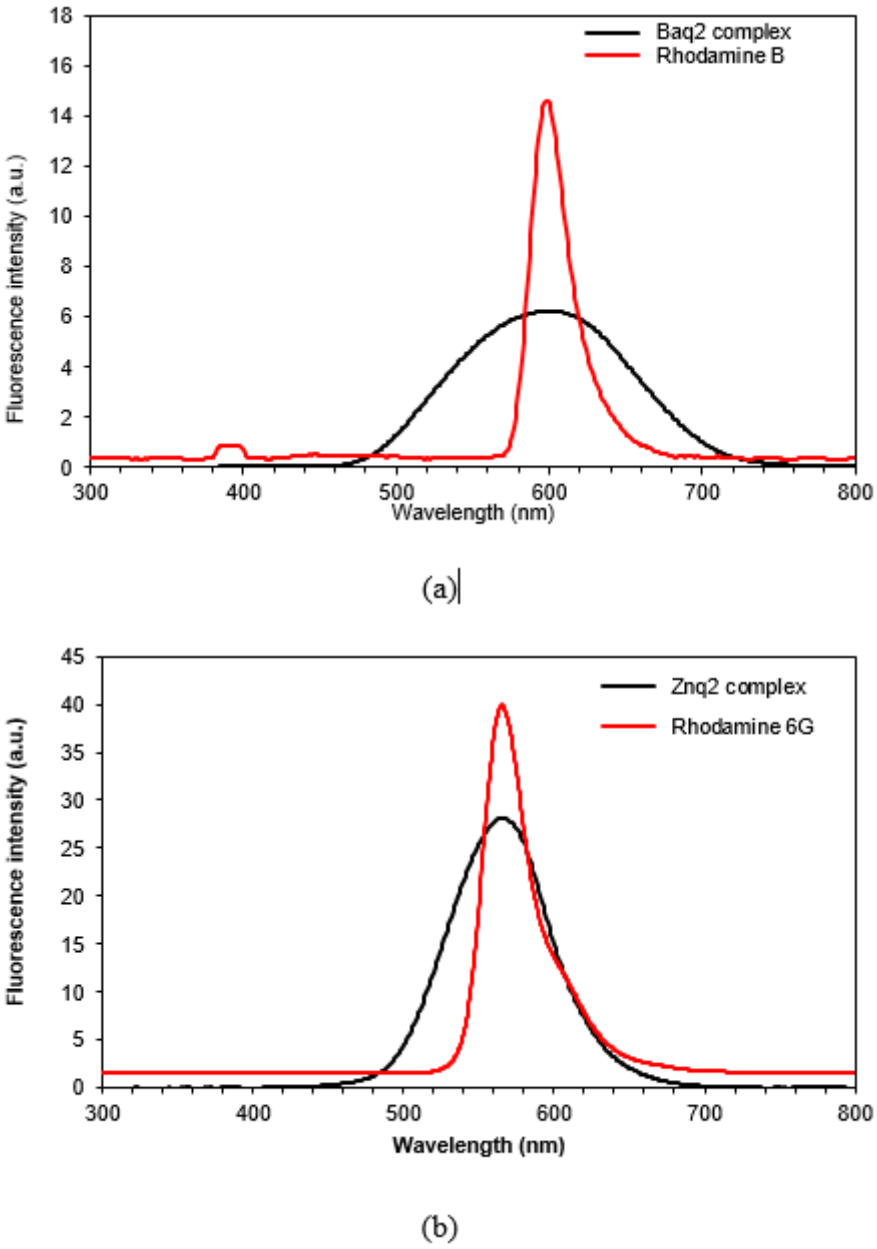

Figure 8

Fluorescence spectra of Baq2 complex (a) and Znq2 complex (b) compared to those of Rhodamine B and Rhodamine 6G, respectively

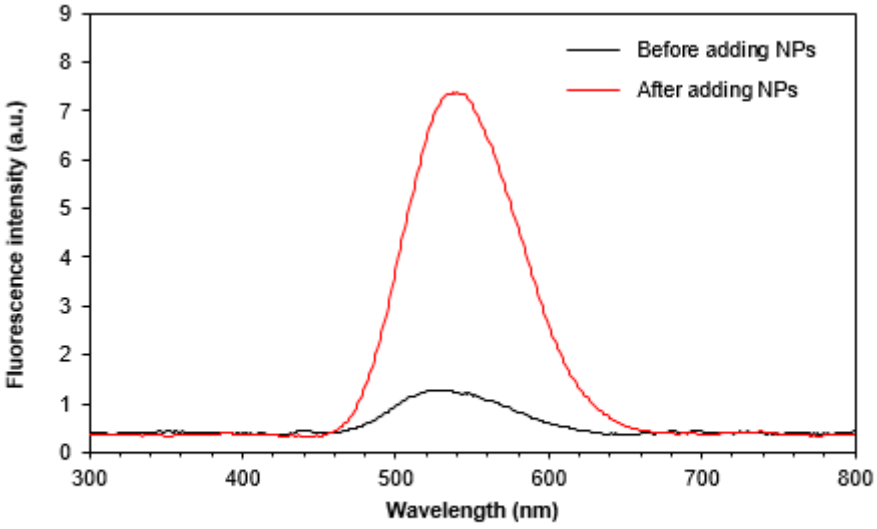

(a) Baq_2

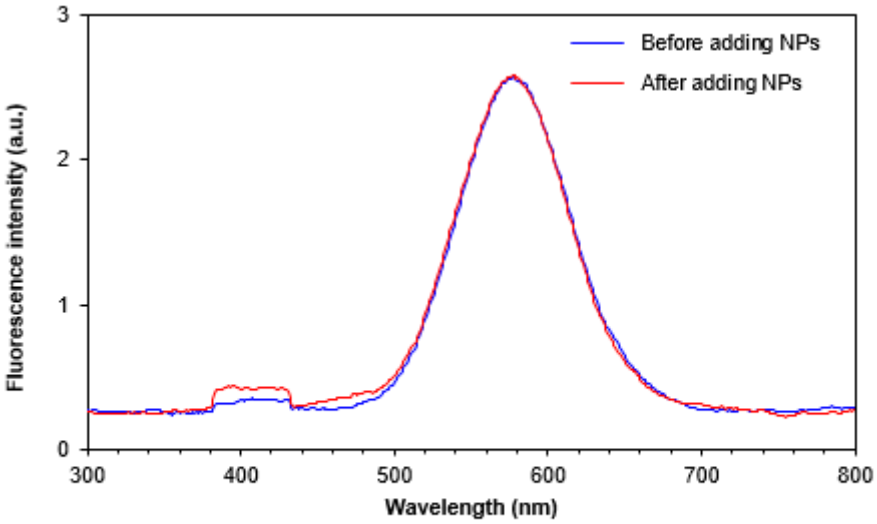

(b) Znq_2

Figure 9

Fluorescence spectra of Baq2 complex (a) and Znq2 complex (b) before and after adding highly-pure nanoparticles